Striatal Alterations of Secretogranin-1, Somatostatin, Prodynorphin, and Cholecystokinin Peptides in an Experimental Mouse Model of Parkinson Disease*[S]

Anna Nilsson‡, Maria Fälth‡, Xiaoqun Zhang§, Kim Kultima‡, Karl Sköld‡, Per Svenningsson§, and Per E. Andrén‡¶

The principal causative pathology of Parkinson disease is the progressive degeneration of dopaminergic neurons in the substantia nigra pars compacta projecting to the striatum in the brain. The information regarding the expression of neuropeptides in parkinsonism is very limited. Here we have elucidated striatal neuropeptide mechanisms in experimental parkinsonism using the unilateral 6-hydroxydopamine model to degenerate dopamine neurons. A thoroughly controlled sample preparation technique together with a peptidomics approach and targeted neuropeptide sequence collections enabled sensitive detection, identification, and relative quantitation of a great number of endogenous neuropeptides. Previously not recognized alterations in neuropeptide levels were identified in the unilateral lesioned mice with or without subchronic 3,4-dihydroxy-L-phenylalanine administration, the conventional treatment of Parkinson disease. Several of these peptides originated from the same precursor such as secretogranin-1, somatostatin, prodynorphin, and cholecystokinin. Disease-related biotransformation of precursors into individual peptides was observed in the experimental model of Parkinson disease. Several previously unreported potentially biologically active peptides were also identified from the striatal samples. This study provides further evidence that neuropeptides take part in mediating the central nervous system failure associated with Parkinson disease. ***Molecular & Cellular Proteomics 8:1094–1104, 2009.***

Parkinson disease (PD)[1] is characterized by progressive loss of dopaminergic neurons in the substantia nigra pars compacta projecting to the striatum in the brain (1). PD symptoms are treated with dopamine (DA) replacement by administration of 3,4-dihydroxy-L-phenylalanine (L-DOPA) and other drugs that stimulate dopaminergic neurotransmission (2, 3). Besides the specific loss of DA content in the striatum, alterations in the transcript and translation of neuropeptides have also been described (4).

Changes in peptide expression may be important in the generation of abnormal basal ganglia activity and the generation of PD symptoms. It is well known that the regulation of opioid peptide synthesis in the basal ganglia is disturbed in parkinsonism. The striatal RNA message for the primary precursor protein of enkephalin, preproenkephalin-A (PPE-A), is increased in parkinsonism, whereas the precursor for dynorphin, preproenkephalin-B (PPE-B), is decreased (5–7). However, the information regarding the expression of neuropeptides from other precursors is very limited in PD.

An important question is the precise identity of which peptides are utilized as co-transmitters in the striatum and how their production is modified in parkinsonism. Almost all previous studies have focused on the regional expression of the mRNA encoding the neuropeptide precursors using *in situ* hybridization. Very little is known regarding the precise identities of the peptide products themselves. This information is important because large precursor molecules (*e.g.* pro-opiomelanocortin) can be processed to produce a variety of neuroactive peptides. If the neuropeptide phenotype of individual striatal output cells can change, this could have important implications for therapeutic strategies because the possible peptide products may act on different receptor types.

The peptidome represents proteolytic processed entities that are derived from protein precursors. These endogenous peptides are often post-translationally modified, typically by C-terminal amidation and/or N-terminal pyroglutamic acidification or acetylation. Conventional techniques like radioimmunoassay (RIA) or Western blot have been used for measuring the differential expression of a number of neuropeptides

From the ‡Department of Pharmaceutical Biosciences, Medical Mass Spectrometry, Uppsala University, SE-75123 Uppsala, Sweden and §Section of Translational Neuropharmacology, Department of Physiology and Pharmacology, Karolinska Institute, SE-17177 Stockholm, Sweden

Received, September 29, 2008, and in revised form, January 7, 2009

Published, MCP Papers in Press, January 8, 2009, DOI 10.1074/mcp.M800454-MCP200

[1] The abbreviations used are: PD, Parkinson disease; ANOVA, analysis of variance; CCK, cholecystokinin; DA, dopamine; L-DOPA, 3,4-dihydroxy-L-phenylalanine; 6-OHDA, 6-hydroxydopamine; PPE-A, preproenkephalin A; PPE-B, preproenkephalin B; RIA, radioimmunoassay; GABA, γ-aminobutyric acid; PEG, polyethylene glycol; CV, coefficient of variance; CSF, cerebrospinal fluid.

in different neurological disorders (8–10). However, although these techniques are sensitive and robust, they are unable to measure several peptides simultaneously, and they can often not distinguish between different neuropeptide variants such as longer or shorter peptide forms or post-translationally modified species.

6-Hydroxydopamine (6-OHDA), a hydroxylated analogue of the natural dopamine neurotransmitter, is one of the most common neurotoxins used to experimentally model nigral dopaminergic degeneration (11, 12). 6-OHDA is commonly injected unilaterally into the ascending medial forebrain bundle, destroying nigral dopaminergic neurons and depleting the ipsilateral striatum of DA levels, hence reproducing the physiopathological features responsible for motor impairments in PD. The model was initially used on rats (13–15) and proved to present clinical features associated with PD also in mice (14, 16, 17).

In the present study, the unilateral 6-OHDA experimental mice model of PD and a peptidomics approach were used to perform a systematic regional analysis of striatal peptides. The striatum is the major input region of the basal ganglia because it receives the majority of afferents from other regions of the brain, especially the cerebral cortex, thalamus, and substantia nigra pars compacta (18). The striatum gives rise to two distinct inhibitory GABAergic projections to the globus pallidus, the so-called direct pathway to the medial globus pallidus and the indirect pathway to the lateral pallidal segment. There is also a direct inhibitory GABAergic pathway from striatum to substantia nigra pars reticulata. Both the direct and indirect pathways also contain specific peptide neuromodulators. The direct pathways contain substance P and opioid peptides derived from PPE-B, and the indirect pathway contains enkephalins derived from PPE-A (for reviews, see Refs. 19 and 20).

Our results showed that a number of identified striatal peptides from different precursors, such as secretogranins, somatostatin, PPE-B, and cholecystokinin (CCK), were significantly altered in unilaterally 6-OHDA-lesioned mice with and without subchronic L-DOPA administration. Additionally several previously unreported potentially novel peptide candidates were identified among the striatal peptides. These peptides had cleavage sites characteristic for neuropeptides and contained post-translational modifications such as phosphorylation and pyroglutamic acid.

EXPERIMENTAL PROCEDURES

Animals, Surgery, and Pharmacological Treatment—The experiments were approved by the local ethics committee at Karolinska Institute (N282/06) and followed the European Communities Council Directive of November, 24 1986 (86/609/EEC). The animals (adult male on a C57BL/6 background (C57BL/6NCrl, strain code 027), n = 12, B&K Universal, Sollentuna, Sweden) were housed in air-conditioned rooms (12-h dark/light cycle) at 20 °C and a humidity of 53%. Mice were anesthetized with ketamine (80 mg/kg, intraperitoneal; Parke-Davis)/xylazine (5 mg/kg, intraperitoneal; Bayer, Kiel, Germany), pretreated with desipramine (25 mg/kg, intraperitoneal; Sigma-Aldrich) and pargyline (5 mg/kg, intraperitoneal; Sigma-Aldrich), placed in a stereotaxic frame, and injected with 6-OHDA (1 μl of a 3 mg/ml solution dissolved in 0.01% ascorbate; Sigma-Aldrich) into the median forebrain bundle of the right hemisphere. The coordinates for injection were: anterior-posterior −1.1 mm, medial-lateral −1.1 mm, and dorsal-ventral −4.75 mm relative to bregma and the dural surface. The injection was at a flow rate of 0.5 μl/min. The injection cannula was left in place for an additional 5 min before being slowly retracted.

Two weeks after unilateral 6-OHDA lesioning, mice were administered apomorphine (1 mg/kg, intraperitoneal; Sigma-Aldrich), and their contralateral rotations were measured over 30 min. Only mice rotating >50 turns/30 min were included in further experiments. One animal did not pass this criterion and was hence excluded from the study. Four weeks after surgery, mice were treated with saline (n = 6) or L-DOPA/benserazide (n = 6; 50/12.5 mg/kg, intraperitoneal; Sigma-Aldrich) once daily for 14 days. The number of ipsi- and contralateral rotations were counted by inspection for 30 min. All mice were killed by focused microwave irradiation using special equipment (Muromachi Kikai, Tokyo, Japan) 15 min after the 15th L-DOPA injection. Striata (left and right) were dissected out for biochemical analyses and stored at −80 C° until further analysis.

Western Blotting—The efficacy of the dopamine denervation was verified post mortem by measurements of the striatal levels of tyrosine hydroxylase as described previously (21). Briefly microwaved frozen tissue samples were sonicated in 1% SDS, transferred to Eppendorf tubes, and boiled for an additional 10 min. Small aliquots of the homogenate were retained for protein determination by the BCA protein assay method (Pierce). Equal amounts of protein (20 μg) were loaded onto 12% acrylamide gels, and the proteins were separated by SDS-PAGE and transferred to nitrocellulose membranes (0.2 mm) (Schleicher & Schuell) by the method of Towbin *et al.* (22). The membranes were immunoblotted using antibodies raised toward tyrosine hydroxylase (Sigma-Aldrich, product number T2928). The antibody binding was revealed by incubation with goat anti-mouse horseradish peroxidase-linked IgG (Pierce, product number 31430, 1:6000–8000 dilution) and the ECL immunoblotting detection system (GE Healthcare).

Sample Preparation—The sample extraction buffer used was 0.25% acetic acid spiked with deuterated Met-enkephalin YGG**F**M (**F** = Phe-d_8), synthesized and purified by HPLC by the Department of Pharmaceutical Chemistry, Organic Chemistry, Uppsala University, Sweden, at a concentration of 40 fmol/μl. The striatal tissue samples, saline-administrated intact side (SAL-INTACT, n = 6), saline-administrated lesioned side (SAL-LESION, n = 6), L-DOPA-administrated intact side (LDOPA-INTACT, n = 6), and L-DOPA-administrated lesioned side (LDOPA-LESION, n = 6) were prepared as described previously (23, 24) with minor modifications. Briefly the peptidergic fraction of the striatal part of the brain was extracted by sonication in 95 °C sample extraction buffer (7.5 μl/mg of tissue) followed by incubation at 95 °C for 1 min. The cell debris were spun down by centrifugation for 40 min at 14 000 × g at 4 °C. The supernatant was transferred to a filtering device (Microcon, YM-10) with a cutoff limit of 10 kDa, and the peptide fraction was isolated through centrifugation for 60 min at 14 000 × g at 4 °C and stored at −80 °C until further analysis.

Liquid Chromatography—The peptide mixture was analyzed on a nano-LC system (Ettan MDLC, GE Healthcare) coupled to an electrospray Q-Tof2 (Waters) or a linear trap quadrupole (LTQ) (Thermo Scientific, San Jose, CA) mass spectrometer. The sample was injected and desalted on a precolumn (300-μm inner diameter × 5 mm, C_{18} PepMapT, 5 μm, 100 Å; LC Packings, Amsterdam, The Netherlands) at a flow rate of 10 μl/min for 10 min. A 15-cm fused silica

emitter with a 75-μm inner diameter and a 375-μm outer diameter (Proxeon Biosystems, Odense, Denmark) was used as the analytical column. The emitter was packed in house with a slurry of reverse-phased Reprosil-Pur C_{18}-AQ 3-μm resin (Dr. Maisch GmbH, Ammerbuch-Entringen, Germany) dispersed in methanol using a pressurized packing device (Proxeon Biosystems). The mobile phases used were Buffer A (0.25% acetic acid in water) and Buffer B (84% ACN and 0.25% acetic acid in water). The peptide samples were separated and eluted during a 40-min gradient from 3 to 60% Buffer B at a flow rate of ~170 nl/min.

Peptide Profiling of the Striatum—The profiling analysis of the peptide samples were performed on the Q-TOF MS instrument. The mass spectrometer was calibrated according to the mass spectrometer manufacturer's recommendations using a PEG solution (PEG 200, 23 ng/μl; PEG 400, 48 ng/μl; and PEG 600, 70 ng/μl; Fluka) delivered from a syringe pump at a flow of 300 nl/min during 2 min. The contact closure feature was used to start the data sampling, and the MS data were acquired in continuous mode in the *m/z* range 300–1000 with a mass resolution of 11,200 (full-width half-maximum) at *m/z* 560.37 ($z = 3$). Mass spectra were collected at a frequency of 4 GHz and integrated into a single spectrum each second. The time between each such spectrum was 0.1 s. Data were collected during 50 min. A reference sample of pooled material was analyzed as every fourth or fifth sample, and in between these runs, one sample from each group of animals (SAL-INTACT, SAL-LESION, LDOPA-INTACT, and LDOPA-LESION) was analyzed in a randomized fashion. Each group of four to five samples was considered as one block in the statistical analysis.

The raw MS data were converted into an ASCII file using the Data Bridge module available in the MassLynx software (Version 3.5, Micromass). These text files were then imported into DeCyder MS2.0 (GE Healthcare) and processed using the import and batch module. Peptide masses were automatically detected in DeCyderMS with the following parameters: peak elution time, 0.4 min; peak resolution, 8000; accepted charge states, 1–12; a signal-to-noise cutoff of 5; and background-subtracted quantification (smooth surface). Manual verification of the detected peptides was performed, and some peptides were removed or added manually in the PepDetect module. The time alignment feature was used to correct for differences in retention times for the samples allowing an adjustment up to 5 min. The aligned intensity maps were then used to match the PepDetect files with a match window of $\pm$1 min and $\pm$0.2 Da. The $\log_2$ intensities from the matched result were exported, and peaks with mass <500 Da or retention time >42 min were removed prior to normalization. On average 655 $\pm$ 13 peaks were found in each sample after filtering.

Relative Quantification of Peptides—Statistical analysis was performed in the language R (Version 2.6.0) (25) using the R/maanova (Version 1.5.1) Bioconductor package (Version 2.1) (26, 27). Linear regression normalization was applied by constructing a median reference file of all the medians of the peak intensities and then applying least squares regression to the scatter plot for each peptide profiling run; this is similar to the approach described by Roy and Becker (28). After normalization only peaks that were detected in at least five of six samples in the four treatment groups were included for further analyses (283 peaks). Missing values were imputed using *k*-nearest neighbors ($k = 10$). On average each sample contained 1.7% missing values prior to imputation.

For each detected peptide, a linear mixed model was utilized using restricted maximum likelihood estimation. Two types of analyses were performed. First, the treatment effect within individuals was estimated. Because the effects of the 6-OHDA lesion can be measured within the same individual, an ANOVA model where samples were set as fixed factors and blocks were set as random factors was used (ANOVA1). This way the individual variation of treatment effects is taken into account. Second, to compare all different treatment effects the data were analyzed using an ANOVA model with the four treatment groups as fixed factors and the samples and blocks as random factors (ANOVA2). Pairwise *t* testing between (SAL-LESION) and (SAL-INTACT), and between (LDOPA-LESION) and (LDOPA-INTACT), and *t* testing between (LDOPA-LESION) and (SAL-LESION) were performed on peptides significant in the ANOVAs. The reference samples were included for estimation of block effects. Significance testing was performed using random permutations of the samples (27, 29) to estimate *p* values for the ANOVA and *t* tests. The function matest() available in the R/maanova package was used. The number of permutations was set to 1000. The estimation of the error variance was accomplished using the James-Stein shrinkage concept, and a test statistic called Fs was used (30). The Fs test has been proven to be robust and perform well under a wide range of assumptions about variance heterogeneity (30). In gene expression studies using microarrays it has been demonstrated to perform acceptably when the variances are truly constant as well when the variances vary from gene to gene (30). This also makes it suitable for LC-MS data. For comparison tabulated *p* values for the observed data using classical F and *t* statistics (only using data from individual peptides) are presented in the supplemental information. The level of statistical significance was set at $p < 0.05$.

Peptide Identification—Nano-LC linear trap quadrupole MS/MS analyses were performed on all the samples for identification of peptides. The same LC setup as above was used, and the MS/MS data were collected in a data-dependent manner. The acquisition was set up to continuously switch between full MS scan (*m/z* 300–2000), zoom scan (most intense peak in full scan), and MS/MS scan (most intense peak in zoom scan) where the most intense peak can be picked twice in a time window of 40 s before being put on an exclusion list during a 150-s period.

The tandem mass spectra generated in the nano-LC-MS/MS run were converted into dta files using Xcalibur (Version 2.0 SR2), and the dta files were then combined into mgf files by using an in-house developed script. Tandem mass spectra were assigned sequences by searching them against three targeted sequence collections: SwePep precursors (123 protein entries), SwePep peptides (245 peptide entries), and SwePep prediction (3,413,034 peptide entries) as described previously (31) using X!Tandem (Version 2006.9.15.4) (32, 33). These targeted sequence collections have been developed using the SwePep database (34) and provide fast, specific, and sensitive identification of endogenous peptides (31). To confirm the identities of previously unreported peptides (not previously identified with mass spectrometry), their corresponding tandem mass spectra were searched against UniProt (48.8) mouse (10,431 protein entries) to check that their tandem mass spectra were not assigned to another sequence in a larger database. The reference sample was searched against UniProt to confirm the sample quality (35).

Tandem mass spectra where one of the three most abundant peaks could correspond to a neural loss of a phosphate group (36) were collected for identification of phosphorylated peptides. The spectra were searched against SwePep precursors allowing for phosphorylations of serine, threonine, and tyrosine, and all hits were manually verified.

The SwePep precursor and the SwePep peptide sequence collections were searched using unspecific cleavage, and the precleaved SwePep predicted sequence collection was searched using no cleavage. The databases were searched using a peptide mass tolerance of $\pm$2 Da and a fragment mass tolerance of $\pm$0.7 Da. The data set was searched with a number of possible post-translational modifications (N-terminal acetylation, N-terminal pyroglutamic acid of glutamine and glutamic acid, C-terminal amidation, and oxidation and dioxidation of methionine and tryptophan). The refinement function in

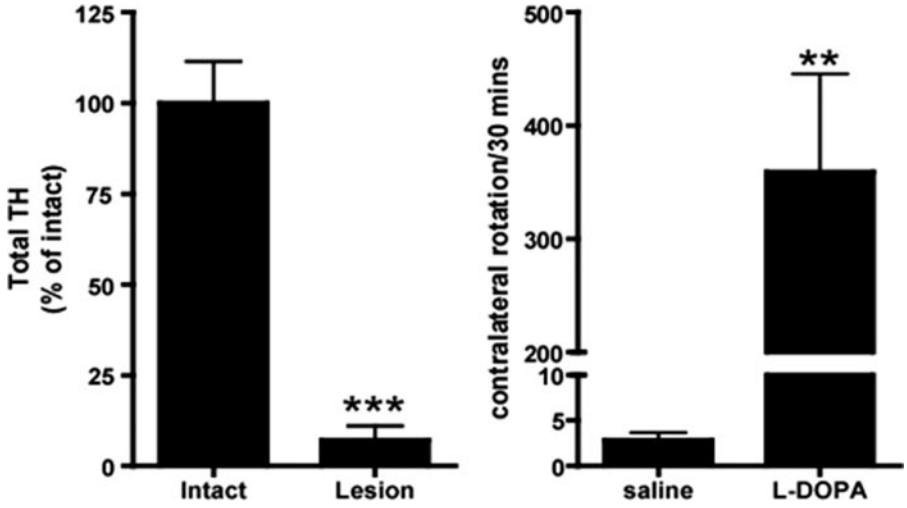

FIG. 1. *A*, reduction of tyrosine hydroxylase (*TH*) in the 6-hydroxydopamine-lesioned side of the striatum compared with intact striatum. The observed reduction was 94%. *B*, number of contralateral rotations during 30 min following saline or L-DOPA administration. Data are expressed as mean ± S.E. **, $p < 0.01$; ***, $p < 0.001$ (paired *t* test). *Error bars* represent standard error of the means.

X!Tandem was used; it allows unspecific cleavage of a precursor if one or more peptides have been identified from it (32). A peptide score with log(*e*) < -2 was considered a significant hit.

The false-positive rate was estimated by searching the reversed sequence collections and calculating the number of hits over a threshold and dividing this number by the number of matches from the targeted sequence collection search (32, 37, 38). If the false-positive rate is over 1% the threshold suggested by the search engine needs to be adjusted for that sequence collection.

RESULTS

Post-mortem Determination of the Efficacy of Unilateral 6-OHDA Lesioning—The efficacy of the unilateral 6-OHDA lesions was evaluated by Western blotting of tyrosine hydroxylase in the striatum. The 6-OHDA lesioning caused a near complete reduction of striatal tyrosine hydroxylase protein (Fig. 1*A*).

Subchronic administration of L-DOPA induced a marked stimulatory effect on contralateral rotational behavior in the unilaterally 6-OHDA-lesioned mice (Fig. 1*B*). This contralateral rotational behavior is known to occur because of stimulation of supersensitive DA receptors in the dopamine-denervated striatum after treatment with L-DOPA or DA agonists (39) only after most dopaminergic nigrostriatal neurons (~90%) have been eliminated (40, 41).

Detected Striatal Peptides and Reproducibility—Following MS analysis and processing with DeCyderMS, more than 200 peaks were automatically detected and matched in all striatal samples. The detected peaks were in the mass range from 300 to 8600 Da with a majority representing masses below 2000 Da. The reference samples, analyzed as every fifth sample in the experimental setup, were used to validate the robustness of the sample analysis. After the linear regression normalization, the median coefficient of variance was reduced by 35%, resulting in a median CV below 4% for peaks detected across all reference samples (in total, CV was calculated for 229 detected peaks across the reference samples, both identified and unidentified, and the median CV among these after normalization was 0.034).

All samples were spiked with 40 fmol/μl deuterated Met-enkephalin. This allowed for an absolute quantitation of endogenous Met-enkephalin. The endogenous levels of Met-enkephalin (260 ± 16 fmol/μl, 1.15 μg/g of tissue) calculated from the levels of spiked deuterated Met-enkephalin correlated well with levels previously measured in striatum (42, 43).

Post-mortem Sample Quality Verification—A peptide from stathmin (stathmin-(2–20)) known to be present in samples where post-mortem degradation has occurred was used as a quality marker in the present study (35). The reference samples were searched against UniProt, and as stathmin-(2–20) was not identified in the database search, the samples were considered to be devoid of protein degradation.

Identified Peptides in Striatum—From the tandem MS analysis of all analyzed samples, there were in total 68 peptides identified by searches against the targeted sequence collections (supplemental table). These peptides were derived from 21 peptide precursors, most of them known to contain neuropeptides. The identified peptides contained several post-translational modifications such as phosphorylation, C-terminal amidation, pyroglutamic acidification, and N-terminal acetylation. Among the identified peptides five were previously unreported (Table I).

Additionally two N-terminal peptides from elongation factor 1-β and two peptides from cerebellin-4 were identified in searches against UniProt. These precursors were not part of the SwePep sequence collections, and therefore the peptides were not identified in those searches.

By matching the experimental masses from the Q-TOF analysis to theoretical peptide masses in SwePep another 19 peptide identities were suggested at the mass accuracy threshold of 0.5 Da (supplemental table). These peptide sequences have so far not been identified above the significance threshold in database searches.

Differentially Expressed Striatal Peptides—To examine how the peptide expression differed in striatum of unilaterally 6-OHDA-lesioned mice treated with saline or L-DOPA, two

TABLE I
Previously unreported peptides identified from striatal tissue extracts

UniProt accession no.	Protein name	Peptide name	Sequence with adjacent cleavage sites	Mass (M + H)	Comment
P22005	PENK_MOUSE	PENK_MOUSE 87–97	KD ↓ ^{87}SSKQDESHLLA^{97} ↓ KK	1214.601	N-terminal part of synenkephalin
		PENK_MOUSE 171–184	KD ↓ ^{171}SHQQESTNNDEDMS^{184} ↓ SKR	1621.603	Part of propeptide
P16014	SCG1_MOUSE	Phosphorylated SCG1_MOUSE 313–330	RR ↓ ^{313}PSPKES(phospho)KEADVATVRLGE^{330} ↓ KR	1992.964	
P60041	SMS_MOUSE	SMS_MOUSE 87–100	EL ↓ ^{87}Pyro-Glu(Q)RSANSNPAMAPRE^{100} ↓ RK	1511.702	
P09240	CCKN_MOUSE	CCKN_MOUSE 21–34	LA ↓ ^{21}Pyro-Glu(Q)PVVPAEATDPVEQ^{34} ↓ RAEEAR	1462.706	N terminus of a propeptide

TABLE II
Striatal peptides found to be differentially regulated

Significant regulations ($p < 0.05$) are marked in bold. Peptides in italic were only identified by mass match. SAL-INTACT, saline-treated intact side; SAL-LESION, saline-treated lesioned side; LDOPA-INTACT, L-DOPA-treated intact side; LDOPA-LESION, L-DOPA-treated lesioned side. lin, linear.

Precursor	Peptide	*p* value		(LDOPA-LESION) − (SAL-LESION) (unpaired *t* test)			(SAL-LESION) − (SAL-INTACT) (paired *t* test)			(LDOPA-LESION) − (LDOPA-INTACT) (paired *t* test)		
		ANOVA1	ANOVA2	Fold change log$_2$	Fold change lin	*p* value	Fold change log$_2$	Fold change lin	*p* value	Fold change log$_2$	Fold change lin	*p* value
P09240 CCKN_MOUSE	^{21}Pyro-Glu(Q)PVVPAEATDPVEQ^{34}	**0.038**	0.075	0.06	1.05	0.712	0.25	1.19	0.155	0.43	1.35	**0.024**
P09240 CCKN_MOUSE	^{2}APSGRMSVLKNLQSLDPSHRISD^{24}	**0.014**	**0.036**	0.48	1.39	0.308	−0.38	0.77	0.336	1.33	2.51	**0.005**
P60041 SMS_MOUSE	^{89}SANSNPAMAPR^{99}	0.052	**0.048**	−0.51	0.70	**0.042**	0.54	1.45	**0.016**	0.05	1.03	0.803
P60041 SMS_MOUSE	^{87}Pyro-Glu(Q)RSANSNPAMAPRE^{100}	**0.018**	**0.020**	−0.63	0.65	0.084	0.71	1.63	**0.006**	0.23	1.17	0.304
P16014 SCG1_MOUSE	^{313}PSPKESKEADVATVRLGE^{330}	**0.035**	0.053	−0.24	0.85	0.255	0.51	1.42	**0.010**	0.03	1.02	0.881
P16014 SCG1_MOUSE	^{419}GRGREPGAHSALDTREE^{435}	**0.011**	**0.009**	−0.24	0.85	0.340	0.68	1.60	**0.017**	0.63	1.55	**0.027**
P16014 SCG1_MOUSE	*^{385}NHPDSELESTANRHGEETEEE^{406}*	**0.026**	0.082	−0.17	0.89	0.549	0.38	1.30	0.130	0.65	1.57	**0.016**
P16014 SCG1_MOUSE	^{457}YPQSKWQEQE^{466}	0.234	**0.037**	−0.32	0.80	**0.033**	0.24	1.18	0.115	0.10	1.07	0.477
P47867 SCG3_MOUSE	^{1}ELSAERPLNEQIAEAEADKI^{20}	**0.003**	**0.015**	0.52	1.44	0.120	−0.50	0.71	0.060	0.94	1.92	**0.002**
O35417 PDYN_MOUSE	^{177}SSEMARDEDGGQDGDQVGHEDLY^{199}	0.715	**0.048**	0.76	1.69	**0.021**	−0.03	0.98	0.920	0.23	1.17	0.415
Q9QXV0 Q9QXV0_MOUSE	^{243}LENPSPQAPA^{252}	**0.038**	0.059	−0.33	0.80	0.230	−0.01	1.00	0.978	−0.58	0.67	**0.011**
Q8BME9 CBLN4_MOUSE	^{66}SKVAFSAVRSTN^{77}	**0.037**	0.065	−0.12	0.92	0.504	−0.20	0.87	0.212	−0.42	0.75	**0.019**
P70296 PEBP1_MOUSE	*^{2}Acetyl-AADISQWAGPL^{12}*	**0.010**	**0.005**	0.03	1.02	0.895	−0.05	0.97	0.833	0.79	1.74	**0.003**
P01193 COLI_MOUSE	*^{222}FKNAIIKNAH^{231}*	**0.007**	**0.029**	0.08	1.05	0.814	0.66	1.58	**0.020**	0.72	1.65	**0.013**
P56388 CART	*^{28}Pyro-Glu(Q)EDAELQPR^{36}*	**0.044**	0.070	−0.31	0.80	0.413	0.65	1.56	**0.013**	0.00	1.00	0.999

statistical ANOVA models were applied to the data set. Paired *t* tests were performed to validate differences due to the 6-OHDA lesioning, and an unpaired *t* test was used to assess the effect of the L-DOPA treatment. The ANOVA model estimating the within-sample effect (ANOVA1) resulted in 12 significantly regulated peptides originating from nine different precursors (Table II). Among these were several peptides derived from the precursors of secretogranins, somatostatin, and CCK. The second ANOVA (ANOVA2) revealed an additional three peptides that were differentially expressed (Table II).

Secretogranin—Secretogranins, also called chromogranins, are a class of acidic secretory proteins that occur in endocrine, neuroendocrine, and neuronal cells. Several known bioactive peptides are derived from this class of proteins (44). In the present study, 14 peptides from secretogranin-1, two from secretogranin-2, and one from secretogranin-3 were identified. From the ANOVAs, four of the peptides from secretogranin-1 and the secretogranin-3-derived peptide were found to be differentially expressed (Table II). The GRGREPGAHSALDTREE peptide was increased on the lesioned side both in animals receiving saline (60%) and L-DOPA (55%). The unphosphorylated form of the potentially bioactive peptide PSPKESKEADVATVRLGE was up-regulated by 42% on the lesioned side of the saline-treated animals, but following L-DOPA administration this increase was reversed. The peptide YPQSKWQEQE, which is part of the GAWK peptide (45), was also affected by the L-DOPA treatment, showing a decrease on the lesioned side of the brain following L-DOPA administration (Table II). The general pattern of expression for all the secretogranin-1-derived peptides was characterized by an increase on the lesioned side of the brain. This trend was especially true for the saline-treated animals, whereas the trend was somewhat more diverse following L-DOPA treatment (Fig. 2).

The peptide derived from the secretogranin-3 precursor displayed a different expression pattern. The level of this peptide was lower on the lesioned side compared with intact side in saline-treated animals, but following L-DOPA administration there was a significant up-regulation in the lesioned side compared with intact side (92%).

Somatostatin—Two peptides derived from somatostatin-28 were found to be differentially expressed. Somatostatin is classified as an inhibitory neurotransmitter that suppresses the release of a range of different hormones such as the gastrointestinal hormones, gastrin, CCK, and secretin. The

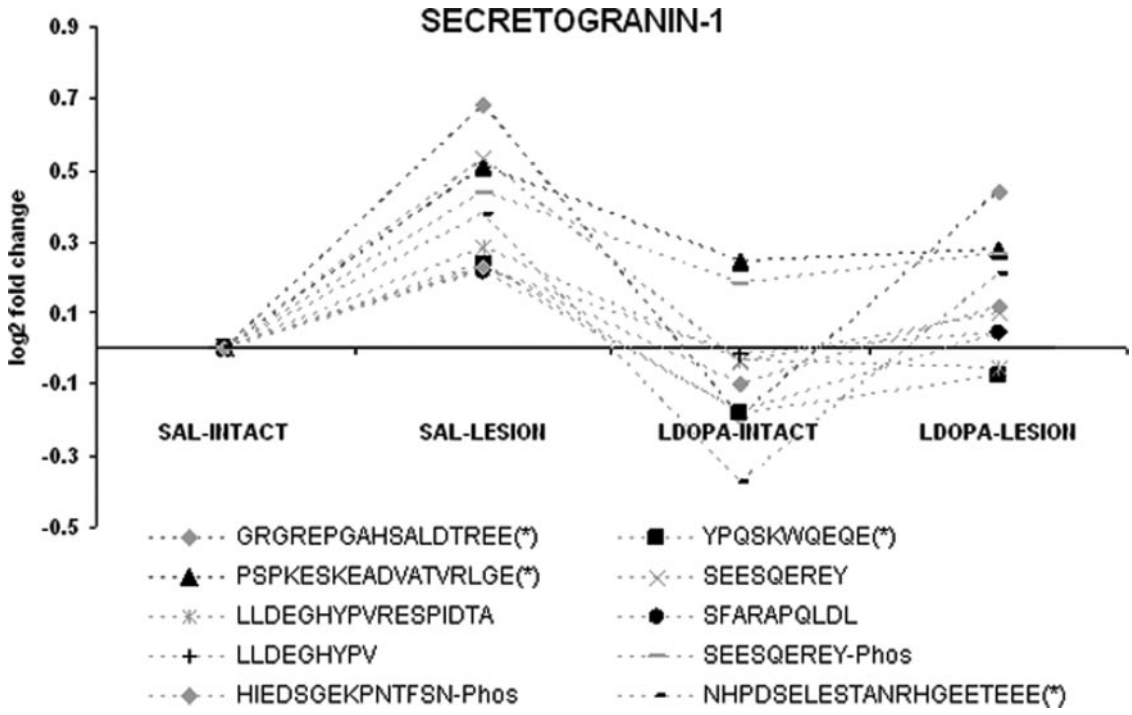

FIG. 2. **The expression profiles of the secretogranin-1-derived peptides.** Each trend *line* represents one individual peptide. The graph presents mean fold changes (log_2) for the striatal peptides levels in the different treatment groups (SAL-LESION, LDOPA-INTACT, and LDOPA-LESION relative to saline-administered intact side SAL-INTACT, which was set to base level (zero)). Peptides showing significant differential expression ($p < 0.05$) are marked with *.

somatostatin-derived peptides were up-regulated on the lesioned side of the brain (45 and 63%, $p < 0.05$, respectively), and following L-DOPA administration the levels were reduced by 30% ($p < 0.05$) and 35% (non-significant) (Table II). Altogether three peptides derived from the N-terminal part of somatostatin-28 and one post-translationally modified prolonged form of the same peptide were identified, and they all had similar expression profiles (Fig. 3). Another somatostatin-derived peptide, AGCKNFFWKTFTSC, displayed a different expression pattern (Fig. 3). However, this peptide was only identified by mass matching. The lack of acceptable MS/MS data might be due to the presence of a disulfide bridge.

Preproenkephalin B—There were in total four peptides identified from the PPE-B precursor. One of these was differentially expressed according to the ANOVA. The peptide SSEMARDEDGGQDGDQVGHEDLY displayed an up-regulation on the lesioned side following L-DOPA treatment (69%) compared with the saline-treated lesioned side. Also in this case all peptides derived from the same precursor had similar expression profiles except for YGGFL (Leu-enkephalin), which is a peptide that is derived from multiple precursors (Fig. 4). The general trend was that L-DOPA treatment increases the expression of PPE-B peptides.

Cholecystokinin—CCK is widespread throughout the central nervous system. It has been suggested to be involved in nausea and anxiety as well as satiating (46, 47). There were two peptides derived from the cholecystokinin precursor that were differentially expressed. These peptides, APSGRMSVLKNLQSLDPSHRISD and pyro-Glu(Q)PVVPAEATDPVEQ, were increased on the L-DOPA-treated lesioned side compared with the intact side of the brain (151 and 35%, respectively) (Table II).

In addition, significant changes in the levels of single peptides from the precursors of phosphatidylethanolamine-binding protein 1 (PEBP1), pro-opiomelanocortin-α, and cocaine- and amphetamine-regulated transcript were found between the lesioned and intact tissue (Table II). Our result did not show any significant pattern of regulation of PPE-A-derived peptides. In line with previous findings, our data indicated a down-regulation of substance P on the lesioned side of the brain, but this change did not reach significance ($p = 0.058$).

DISCUSSION

In the present study a label-free quantitative peptidomics approach was applied to study the relative abundance changes of striatal endogenous peptides in an experimental model of PD with and without L-DOPA administration. The coupling of nano-LC to MS enabled detection and characterization of hundreds of endogenous peptide species simultaneously, and about 70 striatal neuropeptides were unambiguously identified and relatively quantified. Both known and previously unreported peptides derived from precursors such

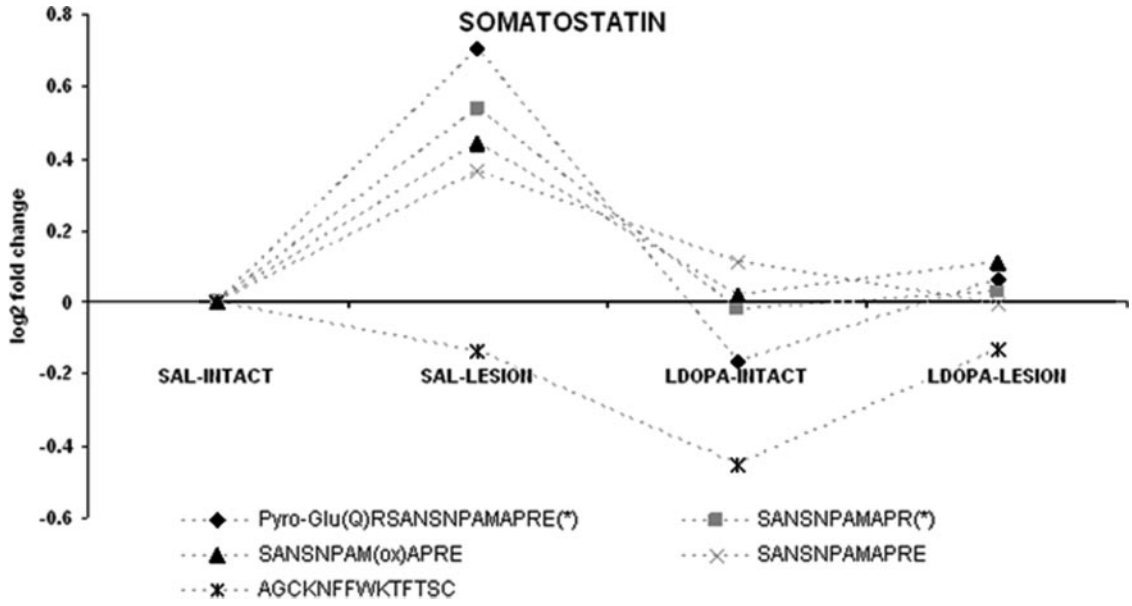

FIG. 3. **The expression profiles of the somatostatin-derived peptides.** Each trend *line* represents one individual peptide. The graph presents mean fold changes (log_2) for the striatal peptides levels in the different treatment groups (SAL-LESION, LDOPA-INTACT, and LDOPA-LESION relative to saline-administered intact side SAL-INTACT, which is set to base level (zero)). Peptides showing significant differential expression ($p < 0.05$) are marked with *.

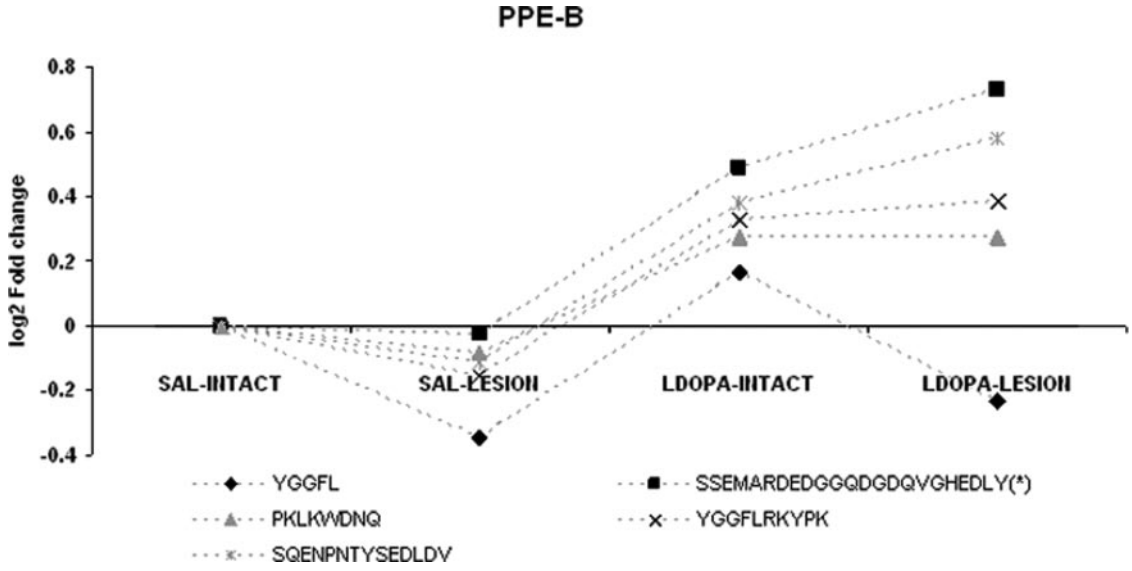

FIG. 4. **The expression profiles of the PPE-B-derived peptides.** Each trend *line* represents one individual peptide. The graph presents mean fold changes (log_2) for the striatal peptides levels in the different treatment groups (SAL-LESION, LDOPA-INTACT, and LDOPA-LESION relative to saline-treated intact side SAL-INTACT, which is set to base level (zero)). Peptides showing significant differential expression ($p < 0.05$) are marked with *.

as secretogranin-1, somatostatin, PPE-B, and CCK were found to be differentially expressed. The present study also addressed the effect on the biotransformation of peptide precursors to peptides, and variations were observed in several precursors after dopamine depletion and L-DOPA administration.

Previously we have measured levels of small proteins in parkinsonian experimental models using profiling and imaging MS technology directly on brain tissue sections (48–50). A number of unique protein expression profile differences were found in the dopamine-denervated side of the brain in specific brain regions when compared with the corresponding intact side, for example, calmodulin, cytochrome *c*, cytochrome *c* oxidase, FKBP-12, ubiquitin, and PEP-19. This technology allowed for the study of complex biochemical processes such as those occurring in experimental PD and provided unique information regarding the peptide and protein expression in selected brain regions. Furthermore we have also showed

that the *in vivo* biotransformation of dynorphin A-(1–17) in the striatum is disturbed in experimental parkinsonism (51).

The 6-OHDA lesion model of PD used in the present study induces a selective, reproducible, and dose-dependent degeneration of nigrostriatal DA neurons (12) and has therefore been extensively used to model PD. Most previous studies have focused on the regional expression of the mRNA encoding the neuropeptide precursors using *in situ* hybridization, but not much is known about the effect on neuropeptide alterations. As individual peptides might target different receptors or different regulatory pathways it is of importance to study the precise identities of the endogenous peptide products. Previous attempts to measure the levels of neuropeptides in parkinsonian experimental models or PD patients have been made using RIA with inconsistent results (9).

Our present results on peptide expression using the 6-OHDA lesion model of PD showed an increase of somatostatin-derived peptides in the DA-denervated striatum. Following L-DOPA administration this pattern of regulation was normalized. Somatostatin is present in substantial amounts in the striatum, particularly in dense plexus of fibers and nerve terminals as well as in cell bodies belonging to a striatal population of medium sized spiny neurons. It acts through somatostatin receptors SST1–5 in the brain (52).

There are several studies indicating a relationship between somatostatin expression and the dopaminergic system. Intracerebroventricular injections of somatostatin increased DA synthesis (53) and release (54), and somatostatin increased DA release from striatal slices (55). Studies on animal models of PD showed an increase of somatostatin mRNA in unilaterally lesioned primates and rats (56, 57). Our present results are in line with the significant increase of somatostatin-like immunoreactivity levels investigated in cerebrospinal fluid (CSF) from 23 patients with untreated early parkinsonian syndrome compared with control subjects (58). However, the opposite was found in CSF of patients with moderate or severe disease (59). Given our data, it may be possible that the increase in somatostatin is a compensatory mechanism trying to restore the DA levels. This is in line with previous work administering DA agonists and an antagonist to rats where increased somatostatin levels were observed following administration of the D2 antagonist haloperidol. Reduced somatostatin levels were detected following co-administration of the two D1 and D2 agonists SKF38393 and quinpirole (60). However, the exact mechanisms of how the different individual somatostatin peptides function remain to be fully characterized.

Furthermore four peptides originating from the secretogranin-1 precursor were differentially expressed. There was a general trend of increased expression in the DA-denervated striatum compared with the intact side. This pattern was then either maintained or reversed following L-DOPA treatment. Secretogranins, also referred to as chromogranins, are present throughout the neuroendocrine system and have been suggested to play an important role in the packaging of hormones and the formation of secretory granules (61, 62) but also to function as precursors of active released peptides (62–64). At least eight secretogranin-1-derived peptides have been identified from different species, and apart from the antibacterial function of secretolytin they all have, to our knowledge, unknown functions (44, 65). Secretogranin-1 has been implicated to be differentially regulated in a number of brain neurological disorders such as schizophrenia (66), multiple sclerosis (67), and Alzheimer disease (68, 69). Additionally rats administrated with reserpine, a drug used for producing an animal model of PD, showed an increase of secretogranin-1 mRNA in substantia nigra pars compacta (70). However, RIA measurements on a secretogranin-1-derived peptide, PE11, in CSF from PD patients did not reveal any alterations compared with control subjects (71).

Our study also showed an increase of the PPE-B-derived peptide, SSEMARDEDGGQDGDQVGHEDLY, following L-DOPA treatment on the lesioned side of the brain. This peptide lacks previous reports of functional characteristics and is annotated as a propeptide sequence. Its pattern of regulation is similar to three other identified peptides derived from the same precursor: α-neoendorphin, the C-terminal part of Dyn-(1–17) (PKLKWDNQ), and the C-terminal part of the precursor (SQENPNTYSEDLDV). These results correlate well with studies performed on striatal PPE-B mRNA levels following L-DOPA treatment in different animal models of PD (7, 72–75). It has been speculated that the increased expression of PPE-B is a key component in the process eventually leading to L-DOPA-induced dyskinesias, the severe side effect associated with L-DOPA treatment (7, 72, 73).

Two cholecystokinin-derived peptides were increased on the lesioned side of the brain following L-DOPA administration. The roles of their individual function remain uncharacterized. DA plays an important role in CCK release, and CCK mRNA levels in the rat striatum have been shown to be elevated following treatment with DA agonists (76). Previously CCK levels have been measured by RIA in 6-OHDA-lesioned rats with or without prolonged L-DOPA treatment, and the L-DOPA treatment increased the CCK immunoreactivity in the lesioned striatum (77). Additionally cholecystokinin peptides have been shown to produce a significant increase of the release of dynorphin B in the neostriatum of the rat and in 6-OHDA-lesioned rats (78). The up-regulation of both CCK- and PPE-B-derived peptides observed in our study following L-DOPA treatment might therefore be related.

The label-free nano-LC-MS quantification approach of peptides used in our study has been shown to perform well compared with methods based on stable isotope labeling (79, 80). There are several advantages of using a label-free method compared with labeling technology. Fewer steps of sample preparation are needed, hence minimizing the loss of peptides during extraction. The cost is reduced because no labeling tags are necessary. A larger part of the peptidome

can be measured because most labeling technologies target only a subset of peptides; *e.g.* ICAT targets Cys-containing peptides (81). Additionally, biologically active peptides are often N- and C-terminally modified and therefore not targeted by amine-specific tagging such as isobaric tags for relative and absolute quantitation (82). On the other hand, the use of stable isotope labeling enables multiplexing, and up to eight samples can be quantified in the same analysis, and ratios representing relative abundances can be extracted directly.

Tissue handling and sample preparation techniques are crucial for obtaining proper quality data in neuropeptide discovery and differential peptidomics. The presence of proteolytic peptides produced post mortem from high abundance proteins has been shown to greatly influence the result and reduce the reproducibility and the quantification (23, 35). A marker for sample degradation such as the peptide stathmin-(2–20) (35) is therefore a valuable tool in assessing the quality of the sample. Obtaining a sample that reflects the true peptidome (without proteolytic peptides produced post mortem) and the use of targeted peptide sequence collections such as those derived from the SwePep database are therefore of great advantage for identifying and quantifying known and new potentially bioactive peptides.

Several recently reported (83) and previously unreported peptides in the present study are likely to have biological function. The peptide PSPKESKEADVATVRLGE derived from secretogranin-1 was found to be increased following DA denervation. It has basic cleavage sites at both the N and C termini and was identified both with (83) and without phosphorylation. Another interesting peptide identified was DADSSVEKQVALLKALYGHGQISH derived from protachykinin (83). It has basic cleavage sites adjacent to both the N and C termini and contains the N-terminal part of neuropeptide K, a peptide well conserved within mammals and known to be biologically active (84). A third previously unreported peptide with potential biological activity is the cholecystokinin-derived peptide pyro-Glu(Q)PVVPAEATDPVEQ, which is the N terminus of its propeptide. The peptide is N-terminally modified and has basic cleavage sites at the C terminus. Obviously MS information alone cannot determine whether a peptide possesses a specific biological function or receptor binding potential. Additional investigations are necessary to elucidate their individual functions and characteristics.

In conclusion, the present data demonstrate that the peptidomics approach used in this study shows a great potential of detecting, identifying, and quantifying the levels of a considerable number of endogenous peptides simultaneously in an animal model of PD. Several of these peptides were differentially regulated including a number of potentially novel peptides. Although alterations in the expression pattern of individual novel peptides or peptide families in different physiological situations can help in suggesting the possible function of a peptide, additional functional characterization studies are needed. Furthermore increased knowledge of the complex relationships among neuropeptides and their interaction partners may make it possible to manipulate the biological system. The aim would be to reduce the problems associated with L-DOPA therapy, such as dyskinesias, and to improve the quality of life of PD patients.

* This work was supported by Swedish Research Council Grants 2004-3417, 621-2007-4686, and 521-2007-3017; the Knut and Alice Wallenberg Foundation, and the Karolinska Institutet Centre for Medical Innovations, Research Program in Medical Bioinformatics.

S The on-line version of this article (available at http://www.mcponline.org) contains supplemental material.

¶ To whom correspondence should be addressed: Dept. of Pharmaceutical Biosciences, Medical Mass Spectrometry, Uppsala University, Box 583 BMC, SE-75123 Uppsala, Sweden. Tel.: 46-18-471-7206; E-mail: per.andren@bmms.uu.se.

REFERENCES

1. Dauer, W., and Przedborski, S. (2003) Parkinson's disease: mechanisms and models. *Neuron* **39,** 889–909
2. Cotzias, G. C. (1968) L-Dopa for Parkinsonism. *N. Engl. J. Med.* **278,** 630
3. Fahn, S., Oakes, D., Shoulson, I., Kieburtz, K., Rudolph, A., Lang, A., Olanow, C. W., Tanner, C., and Marek, K. (2004) Levodopa and the progression of Parkinson's disease. *N. Engl. J. Med.* **351,** 2498–2508
4. Gilgun-Sherki, Y., Hellmann, M., Melamed, E., and Offen, D. (2004) The role of neurotransmitters and neuropeptides in Parkinson's disease: implications for therapy. *Drugs Future* **29,** 1261–1272
5. Duty, S., Henry, B., Crossman, A. R., and Brotchie, J. M. (1998) Topographical organization of opioid peptide precursor gene expression following repeated apomorphine treatment in the 6-hydroxydopamine-lesioned rat. *Exp. Neurol.* **150,** 223–234
6. Gross, C. E., Ravenscroft, P., Dovero, S., Jaber, M., Bioulac, B., and Bezard, E. (2003) Pattern of levodopa-induced striatal changes is different in normal and MPTP-lesioned mice. *J. Neurochem.* **84,** 1246–1255
7. Henry, B., Crossman, A. R., and Brotchie, J. M. (1999) Effect of repeated L-DOPA, bromocriptine, or lisuride administration on preproenkephalin-A and preproenkephalin-B mRNA levels in the striatum of the 6-hydroxydopamine-lesioned rat. *Exp. Neurol.* **155,** 204–220
8. Buck, S. H., Burks, T. F., Brown, M. R., and Yamamura, H. I. (1981) Reduction in basal ganglia and substantia nigra substance P levels in Huntington's disease. *Brain Res.* **209,** 464–469
9. Fernandez, A., de Ceballos, M. L., Rose, S., Jenner, P., and Marsden, C. D. (1996) Alterations in peptide levels in Parkinson's disease and incidental Lewy body disease. *Brain* **119,** 823–830
10. Franceschi, M., Perego, L., Ferini-Strambi, L., Smirne, S., and Canal, N. (1988) Neuroendocrinological function in Alzheimer's disease. *Neuroendocrinology* **48,** 367–370
11. Simola, N., Morelli, M., and Carta, A. R. (2007) The 6-hydroxydopamine model of Parkinson's disease. *Neurotox. Res.* **11,** 151–167
12. Ungerstedt, U. (1968) 6-Hydroxy-dopamine induced degeneration of central monoamine neurons. *Eur. J. Pharmacol.* **5,** 107–110
13. Breese, G. R., and Traylor, T. D. (1972) Developmental characteristics of brain catecholamines and tyrosine hydroxylase in the rat: effects of 6-hydroxydopamine. *Br. J. Pharmacol.* **44,** 210–222
14. Zhang, X., Andren, P. E., Greengard, P., and Svenningsson, P. (2008) Evidence for a role of the 5-HT1B receptor and its adaptor protein, p11, in L-DOPA treatment of an animal model of Parkinsonism. *Proc. Natl. Acad. Sci. U. S. A.* **105,** 2163–2168
15. Ungerstedt, U., and Arbuthnott, G. W. (1970) Quantitative recording of rotational behavior in rats after 6-hydroxy-dopamine lesions of the nigrostriatal dopamine system. *Brain Res.* **24,** 485–493
16. Akerud, P., Canals, J. M., Snyder, E. Y., and Arenas, E. (2001) Neuroprotection through delivery of glial cell line-derived neurotrophic factor by neural stem cells in a mouse model of Parkinson's disease. *J. Neurosci.* **21,** 8108–8118
17. Lundblad, M., Picconi, B., Lindgren, H., and Cenci, M. A. (2004) A model of L-DOPA-induced dyskinesia in 6-hydroxydopamine lesioned mice:

relation to motor and cellular parameters of nigrostriatal function. *Neurobiol. Dis.* **16,** 110–123
18. Albin, R. L., Young, A. B., and Penney, J. B. (1989) The functional anatomy of basal ganglia disorders. *Trends Neurosci.* **12,** 366–375
19. Obeso, J. A., Rodriguez-Oroz, M. C., Rodriguez, M., Lanciego, J. L., Artieda, J., Gonzalo, N., and Olanow, C. W. (2000) Pathophysiology of the basal ganglia in Parkinson's disease. *Trends Neurosci.* **23,** S8–19
20. Wichmann, T., and DeLong, M. R. (1996) Functional and pathophysiological models of the basal ganglia. *Curr. Opin. Neurobiol.* **6,** 751–758
21. Svenningsson, P., Chergui, K., Rachleff, I., Flajolet, M., Zhang, X., El Yacoubi, M., Vaugeois, J. M., Nomikos, G. G., and Greengard, P. (2006) Alterations in 5-HT1B receptor function by p11 in depression-like states. *Science* **311,** 77–80
22. Towbin, H., Staehelin, T., and Gordon, J. (1979) Electrophoretic transfer of proteins from polyacrylamide gels to nitrocellulose sheets: procedure and some applications. *Proc. Natl. Acad. Sci. U. S. A.* **76,** 4350–4354
23. Skold, K., Svensson, M., Kaplan, A., Bjorkesten, L., Astrom, J., and Andren, P. E. (2002) A neuroproteomic approach to targeting neuropeptides in the brain. *Proteomics* **2,** 447–454
24. Svensson, M., Skold, K., Svenningsson, P., and Andren, P. E. (2003) Peptidomics-based discovery of novel neuropeptides. *J. Proteome Res.* **2,** 213–219
25. R Development Core Team (2006) *R: a Language and Environment for Statistical Computing*, R Foundation for Statistical Computing, Vienna, Austria
26. Gentleman, R. C., Carey, V. J., Bates, D. M., Bolstad, B., Dettling, M., Dudoit, S., Ellis, B., Gautier, L., Ge, Y., Gentry, J., Hornik, K., Hothorn, T., Huber, W., Iacus, S., Irizarry, R., Leisch, F., Li, C., Maechler, M., Rossini, A. J., Sawitzki, G., Smith, C., Smyth, G., Tierney, L., Yang, J. Y., and Zhang, J. (2004) Bioconductor: open software development for computational biology and bioinformatics. *Genome Biol.* **5,** R80
27. Wu, H., Yang, H., Churchill, G., Kerr, K., and Cui, X. (2007) *Maanova: Tools for Analyzing Micro Array Experiments*, R package version 1.8.0, Bioconductor, Seattle, WA
28. Roy, S. M., and Becker, C. H. (2007) Quantification of proteins and metabolites by mass spectrometry without isotopic labeling. *Methods Mol. Biol.* **359,** 87–105
29. Good, P. (2000) *Permutation Tests: a Practical Guide to Resampling Methods for Testing Hypotheses*, 2nd Ed., Springer-Verlag, New York
30. Cui, X., Hwang, J. T., Qiu, J., Blades, N. J., and Churchill, G. A. (2005) Improved statistical tests for differential gene expression by shrinking variance components estimates. *Biostatistics* (*Oxf.*) **6,** 59–75
31. Falth, M., Skold, K., Svensson, M., Nilsson, A., Fenyo, D., and Andren, P. E. (2007) Neuropeptidomics strategies for specific and sensitive identification of endogenous peptides. *Mol. Cell. Proteomics* **6,** 1188–1197
32. Craig, R., and Beavis, R. C. (2003) A method for reducing the time required to match protein sequences with tandem mass spectra. *Rapid Commun. Mass Spectrom.* **17,** 2310–2316
33. Craig, R., and Beavis, R. C. (2004) TANDEM: matching proteins with tandem mass spectra. *Bioinformatics* **20,** 1466–1467
34. Falth, M., Skold, K., Norrman, M., Svensson, M., Fenyo, D., and Andren, P. E. (2006) SwePep, a database designed for endogenous peptides and mass spectrometry. *Mol. Cell. Proteomics* **5,** 998–1005
35. Skold, K., Svensson, M., Norrman, M., Sjogren, B., Svenningsson, P., and Andren, P. E. (2007) The significance of biochemical and molecular sample integrity in brain proteomics and peptidomics: stathmin 2–20 and peptides as sample quality indicators. *Proteomics* **7,** 4445–4456
36. Kocher, T., Savitski, M. M., Nielsen, M. L., and Zubarev, R. A. (2006) PhosTShunter: a fast and reliable tool to detect phosphorylated peptides in liquid chromatography Fourier transform tandem mass spectrometry data sets. *J. Proteome Res.* **5,** 659–668
37. Moore, R. E., Young, M. K., and Lee, T. D. (2002) Qscore: an algorithm for evaluating SEQUEST database search results. *J. Am. Soc. Mass Spectrom.* **13,** 378–386
38. Peng, J., Elias, J. E., Thoreen, C. C., Licklider, L. J., and Gygi, S. P. (2003) Evaluation of multidimensional chromatography coupled with tandem mass spectrometry (LC/LC-MS/MS) for large-scale protein analysis: the yeast proteome. *Journal. of Proteome Res.* **2,** 43–50
39. Ungerstedt, U. (1976) 6-Hydroxydopamine-induced degeneration of the nigrostriatal dopamine pathway: the turning syndrome. *Pharmacol. Ther.* **2,** 37–40
40. Deumens, R., Blokland, A., and Prickaerts, J. (2002) Modeling Parkinson's disease in rats: an evaluation of 6-OHDA lesions of the nigrostriatal pathway. *Exp. Neurol.* **175,** 303–317
41. Hefti, F., Melamed, E., Sahakian, B. J., and Wurtman, R. J. (1980) Circling behavior in rats with partial, unilateral nigro-striatal lesions: effect of amphetamine, apomorphine, and DOPA. *Pharmacol. Biochem. Behav.* **12,** 185–188
42. Bohan, T. P., and Meek, J. L. (1978) Met-enkephalin: rapid separation from brain extracts using high-pressure liquid chromatography, and quantitation by binding assay. *Neurochem. Res.* **3,** 367–372
43. Yang, H. Y., Hong, J. S., and Costa, E. (1977) Regional distribution of LEU and MET enkephalin in rat brain. *Neuropharmacology* **16,** 303–307
44. Montero-Hadjadje, M., Vaingankar, S., Elias, S., Tostivint, H., Mahata, S. K., and Anouar, Y. (2008) Chromogranins A and B and secretogranin II: evolutionary and functional aspects. *Acta Physiol.* (*Oxf.*) **192,** 309–324
45. Benjannet, S., Leduc, R., Lazure, C., Seidah, N. G., Marcinkiewicz, M., and Chretien, M. (1985) GAWK, a novel human pituitary polypeptide: isolation, immunocytochemical localization and complete amino acid sequence. *Biochem. Biophys. Res. Commun.* **126,** 602–609
46. Gibbs, J., Young, R. C., and Smith, G. P. (1973) Cholecystokinin decreases food intake in rats. *J. Comp. Physiol. Psychol.* **84,** 488–495
47. Greenough, A., Cole, G., Lewis, J., Lockton, A., and Blundell, J. (1998) Untangling the effects of hunger, anxiety, and nausea on energy intake during intravenous cholecystokinin octapeptide (CCK-8) infusion. *Physiol. Behav.* **65,** 303–310
48. Pierson, J., Norris, J. L., Aerni, H. R., Svenningsson, P., Caprioli, R. M., and Andren, P. E. (2004) Molecular profiling of experimental Parkinson's disease: direct analysis of peptides and proteins on brain tissue sections by MALDI mass spectrometry. *J. Proteome Res.* **3,** 289–295
49. Pierson, J., Svenningsson, P., Caprioli, R. M., and Andren, P. E. (2005) Increased levels of ubiquitin in the 6-OHDA-lesioned striatum of rats. *J. Proteome Res.* **4,** 223–226
50. Skold, K., Svensson, M., Nilsson, A., Zhang, X., Nydahl, K., Caprioli, R. M., Svenningsson, P., and Andren, P. E. (2006) Decreased striatal levels of PEP-19 following MPTP lesion in the mouse. *J. Proteome Res.* **5,** 262–269
51. Klintenberg, R., and Andren, P. E. (2005) Altered extracellular striatal in vivo biotransformation of the opioid neuropeptide dynorphin A(1–17) in the unilateral 6-OHDA rat model of Parkinson's disease. *J. Mass Spectrom.* **40,** 261–270
52. Aguado-Llera, D., Puebla-Jimenez, L., Yebenes-Gregorio, L., and Arilla-Ferreiro, E. (2007) Alteration of the somatostatinergic system in the striatum of rats with acute experimental autoimmune encephalomyelitis. *Neuroscience* **148,** 238–249
53. Garcia-Sevilla, J. A., Magnusson, T., and Carlsson, A. (1978) Effect of intracerebroventricularly administered somatostatin on brain monoamine turnover. *Brain Res.* **155,** 159–164
54. Rakovska, A., Javitt, D., Raichev, P., Ang, R., Balla, A., Aspromonte, J., and Vizi, S. (2003) Physiological release of striatal acetylcholine (in vivo): effect of somatostatin on dopaminergic-cholinergic interaction. *Brain Res. Bull.* **61,** 529–536
55. Chesselet, M. F., and Reisine, T. D. (1983) Somatostatin regulates dopamine release in rat striatal slices and cat caudate nuclei. *J. Neurosci.* **3,** 232–236
56. Eve, D. J., Nisbet, A. P., Kingsbury, A. E., Temlett, J., Marsden, C. D., and Foster, O. J. (1997) Selective increase in somatostatin mRNA expression in human basal ganglia in Parkinson's disease. *Brain Res. Mol. Brain Res.* **50,** 59–70
57. Rajakumar, N., Rushlow, W., Rajakumar, B., Naus, C. C., Stoessl, A. J., and Flumerfelt, B. A. (1997) Effects of graft-derived dopaminergic innervation on the target neurons of patch and matrix compartments of the striatum. *Neuroscience* **76,** 1173–1185
58. Espino, A., Ambrosio, S., Bartrons, R., Bendahan, G., and Calopa, M. (1994) Cerebrospinal monoamine metabolites and amino acid content in patients with parkinsonian syndrome and rats lesioned with MPP+. *J. Neural Transm. Park. Dis. Dement. Sect.* **7,** 167–176
59. Strittmatter, M., Hamann, G. F., Strubel, D., Cramer, H., and Schimrigk, K. (1996) Somatostatin-like immunoreactivity, its molecular forms and monoaminergic metabolites in aged and demented patients with Parkinson's disease—effect of L-Dopa. *J. Neural Transm.* **103,** 591–602
60. Marin, C., Engber, T. M., Bonastre, M., Chase, T. N., and Tolosa, E. (1996)

Effect of long-term haloperidol treatment on striatal neuropeptides: relation to stereotyped behavior. *Brain Res.* **731,** 57–62
61. Helle, K. B. (2004) The granin family of uniquely acidic proteins of the diffuse neuroendocrine system: comparative and functional aspects. *Biol. Rev. Camb. Philos. Soc.* **79,** 769–794
62. Taupenot, L., Harper, K. L., and O'Connor, D. T. (2003) The chromogranin-secretogranin family. *N. Engl. J. Med.* **348,** 1134–1149
63. Eiden, L. E. (1987) Is chromogranin a prohormone? *Nature* **325,** 301
64. Fischer-Colbrie, R., Laslop, A., and Kirchmair, R. (1995) Secretogranin II: molecular properties, regulation of biosynthesis and processing to the neuropeptide secretoneurin. *Prog. Neurobiol.* **46,** 49–70
65. Nielsen, E., Welinder, B. S., and Madsen, O. D. (1991) Chromogranin-B, a putative precursor of eight novel rat glucagonoma peptides through processing at mono-, di-, or tribasic residues. *Endocrinology* **129,** 3147–3156
66. Landen, M., Grenfeldt, B., Davidsson, P., Stridsberg, M., Regland, B., Gottfries, C. G., and Blennow, K. (1999) Reduction of chromogranin A and B but not C in the cerebrospinal fluid in subjects with schizophrenia. *Eur. Neuropsychopharmacol.* **9,** 311–315
67. Mattsson, N., Ruetschi, U., Podust, V. N., Stridsberg, M., Li, S., Andersen, O., Haghighi, S., Blennow, K., and Zetterberg, H. (2007) Cerebrospinal fluid concentrations of peptides derived from chromogranin B and secretogranin II are decreased in multiple sclerosis. *J. Neurochem.* **103,** 1932–1939
68. Lechner, T., Adlassnig, C., Humpel, C., Kaufmann, W. A., Maier, H., Reinstadler-Kramer, K., Hinterholzl, J., Mahata, S. K., Jellinger, K. A., and Marksteiner, J. (2004) Chromogranin peptides in Alzheimer's disease. *Exp. Gerontol.* **39,** 101–113
69. Marksteiner, J., Lechner, T., Kaufmann, W. A., Gurka, P., Humpel, C., Nowakowski, C., Maier, H., and Jellinger, K. A. (2000) Distribution of chromogranin B-like immunoreactivity in the human hippocampus and its changes in Alzheimer's disease. *Acta Neuropathol.* **100,** 205–212
70. Mahata, S. K., Mahata, M., Fischer-Colbrie, R., and Winkler, H. (1993) Reserpine causes differential changes in the mRNA levels of chromogranin B, secretogranin II, carboxypeptidase H, α-amidating monooxygenase, the vesicular amine transporter and of synaptin/synaptophysin in rat brain. *Brain Res. Mol. Brain Res.* **19,** 83–92
71. Eder, U., Leitner, B., Kirchmair, R., Pohl, P., Jobst, K. A., Smith, A. D., Mally, J., Benzer, A., Riederer, P., Reichmann, H., Saria, A., and Winkler, H. (1998) Levels and proteolytic processing of chromogranin A and B and secretogranin II in cerebrospinal fluid in neurological diseases. *J. Neural Transm.* **105,** 39–51
72. Cenci, M. A., Lee, C. S., and Bjorklund, A. (1998) L-DOPA-induced dyskinesia in the rat is associated with striatal overexpression of prodynorphin- and glutamic acid decarboxylase mRNA. *Eur. J. Neurosci.* **10,** 2694–2706
73. Ravenscroft, P., Chalon, S., Brotchie, J. M., and Crossman, A. R. (2004) Ropinirole versus L-DOPA effects on striatal opioid peptide precursors in a rodent model of Parkinson's disease: implications for dyskinesia. *Exp. Neurol.* **185,** 36–46
74. St-Hilaire, M., Landry, E., Levesque, D., and Rouillard, C. (2005) Denervation and repeated L-DOPA induce complex regulatory changes in neurochemical phenotypes of striatal neurons: implication of a dopamine D1-dependent mechanism. *Neurobiol. Dis.* **20,** 450–460
75. Tel, B. C., Zeng, B. Y., Cannizzaro, C., Pearce, R. K., Rose, S., and Jenner, P. (2002) Alterations in striatal neuropeptide mRNA produced by repeated administration of L-DOPA, ropinirole or bromocriptine correlate with dyskinesia induction in MPTP-treated common marmosets. *Neuroscience* **115,** 1047–1058
76. Ding, X. Z., and Mocchetti, I. (1992) Dopaminergic regulation of cholecystokinin mRNA content in rat striatum. *Brain Res. Mol. Brain Res.* **12,** 77–83
77. Taylor, M. D., De Ceballos, M. L., Rose, S., Jenner, P., and Marsden, C. D. (1992) Effects of a unilateral 6-hydroxydopamine lesion and prolonged L-3,4-dihydroxyphenylalanine treatment on peptidergic systems in rat basal ganglia. *Eur. J. Pharmacol.* **219,** 183–192
78. You, Z. B., Herrera-Marschitz, M., Pettersson, E., Nylander, I., Goiny, M., Shou, H. Z., Kehr, J., Godukhin, O., Hokfelt, T., Terenius, L., and Ungerstedt, U. (1996) Modulation of neurotransmitter release by cholecystokinin in the neostriatum and substantia nigra of the rat: regional and receptor specificity. *Neuroscience* **74,** 793–804
79. Asara, J. M., Christofk, H. R., Freimark, L. M., and Cantley, L. C. (2008) A label-free quantification method by MS/MS TIC compared to SILAC and spectral counting in a proteomics screen. *Proteomics* **8,** 994–999
80. Turck, C. W., Falick, A. M., Kowalak, J. A., Lane, W. S., Lilley, K. S., Phinney, B. S., Weintraub, S. T., Witkowska, H. E., and Yates, N. A. (2007) The Association of Biomolecular Resource Facilities Proteomics Research Group 2006 study: relative protein quantitation. *Mol. Cell. Proteomics* **6,** 1291–1298
81. Gygi, S. P., Rist, B., Gerber, S. A., Turecek, F., Gelb, M. H., and Aebersold, R. (1999) Quantitative analysis of complex protein mixtures using isotope-coded affinity tags. *Nat. Biotechnol.* **17,** 994–999
82. Zieske, L. R. (2006) A perspective on the use of iTRAQ reagent technology for protein complex and profiling studies. *J. Exp. Bot.* **57,** 1501–1508
83. Zhang, X., Che, F. Y., Berezniuk, I., Sonmez, K., Toll, L., and Fricker, L. D. (2008) Peptidomics of Cpe(fat/fat) mouse brain regions: implications for neuropeptide processing. *J. Neurochem.* **107,** 1596–1613
84. Tatemoto, K., Lundberg, J. M., Jornvall, H., and Mutt, V. (1985) Neuropeptide K: isolation, structure and biological activities of a novel brain tachykinin. *Biochem. Biophys. Res. Commun.* **128,** 947–953